

Cite this: *Green Chem.*, 2011, **13**, 1311

www.rsc.org/greenchem

PAPER

Preparation of a Cu–Ru/carbon nanotube catalyst for hydrogenolysis of glycerol to 1,2-propanediol *via* hydrogen spillover†

Zhijie Wu, Yuzhen Mao, Xiaoxiao Wang and Minghui Zhang*

Received 14th November 2010, Accepted 28th January 2011

DOI: 10.1039/c0gc00809e

A Cu–Ru nanoparticle catalyst supported on carbon nanotubes was prepared by a chemical replacement reaction between Cu metal nanoparticles and Ru³⁺ cations. The as-prepared catalyst was characterized by X-ray diffraction, X-ray photoelectron spectroscopy, H₂ and CO chemisorption, and transmission electron microscopy. The results showed that the highly dispersed Ru clusters were present on the external surface of the Cu particles. These tiny Ru clusters did not activate glycerol to carry its hydrogenolysis, but instead activated and generated active hydrogen, which was transferred to the Cu surface nearby *via* hydrogen spillover. The Cu–Ru catalyst exhibited selectivity for 1,2-propanediol that was as high as Cu metal, and much higher hydrogenolysis activity than pure Cu metal because of the hydrogen spillover effect, which benefited from the Ru clusters.

Introduction

Glycerol is an attractive resource because of its ample availability as a by-product formed in biodiesel production, and because it is a model compound that allows not only the exploration of its conversion to H₂ and CO₂, but also details of the chemical transformations to other alcohols, such as 1,2-propanediol (1,2-PDO) and 1,3-propanediol (1,3-PDO).¹ It has been reported that glycerol can be converted to propanediols by hydrogenolysis using heterogeneous catalysts.² This reaction is currently widely studied because it is an important and appropriate probe for studying the selective removal of excess hydroxyl groups present in biofeedstocks (*i.e.*, sugars and sugar alcohols), which is important for the formation of fuels and chemicals with lower oxygen content.^{3,4}

Cu metal catalysts generally possess a high selectivity for producing 1,2-propanediol,⁵ because of their intrinsic ability to selectively cleave the C–O bonds in preference to the C–C bonds in glycerol,⁴ which is required for propylene glycol formation, suggesting higher hydrogenation activity toward C–O bond than hydrogenolysis activity.⁶ To increase the activity of Cu metal, Cu-based bimetallic catalysts (Cu–Cr,^{7a,7b} Cu–Al^{7c} and Cu–Ag^{7d}) were developed to promote the cleavage of C–O bonds and the hydrogen activation capability of Cu metal. By comparison,

Group VIII metals, such as Ru metal catalysts,⁸ are well known to be very active in direct cleavage C–C and C–O bonds and be active in the hydrogenolysis of glycerol. Unfortunately, Ru often promotes excessive C–C cleavage, resulting in a high selectivity for hydrocarbons (mainly methane).⁶ Ru surface-modified by sulfur has been reported to promote the selectivity for 1,2-propanediol by poisoning the active Ru sites and changing their selectivity towards the cleavage of C–C bonds.⁶

Another report on the poisoning of C–C bond hydrogenolysis active sites describes the deposition of Ru clusters on the surface of copper by the redox reduction of Cu metal with RuCl₃ solution. A new catalytic site, Cu_xRu_yCl_z on the high index planes of Cu, was formed and exhibited high activity and selectivity.⁶ At present, bimetallic metal catalysts, especially Cu-based⁷ and Ru-based⁹ catalysts, have attracted increasing interest for their ability to promote the performance of glycerol hydrogenolysis.

Recently, a highly active and selective Ru–Cu bimetallic catalyst supported on clay has been reported for the hydrogenolysis of glycerol to 1,2-propanediol.¹⁰ The Ru–Cu catalyst was prepared by covering Ru metal with Cu metal by impregnation, suggesting the requirement of modification of the Ru surface to promote the selectivity. In our previous work, another route for the surface modification of metal nanoparticles with added metals has been studied by the chemical replacement method,¹¹ and the surface alloying/interaction of host metal and added metals was revealed to promote the hydrogenation activity. In our view, the surface modification of Cu nanoparticles by Ru metal may combine the high selectivity of Cu metal and high hydrogenation activity of Ru metal, which results in a good bimetallic catalyst for glycerol hydrogenolysis. In addition, carbon materials are

Institute of New Catalytic Materials Science, Department of Material Chemistry, College of Chemistry, and Key Laboratory of Advanced Energy Materials Chemistry (MOE), Nankai University, Tianjin, 300071, China. E-mail: zhangmh@nankai.edu.cn; Fax: +86 22-2350-7730; Tel: +86 22-2350-7730

† Electronic supplementary information (ESI) available: Fig. S1 and Table S1. See DOI: 10.1039/c0gc00809e

Table 1 The surface properties, metal loadings and metal dispersions of catalysts

Sample	S_{BET}^a (m ² g ⁻¹)	V_{pore}^b (cm ³ g ⁻¹)	D_{ave}^c (nm)	Metal loading (wt.%)	Metal dispersion (d_{chem} , nm) ^d	
					Ru	Cu
Ru/C	—	—	—	5.0 (Ru)	0.19 (5.7)	—
MWCNTs	135.8	0.31	10.8	—	—	—
Cu/MWCNTs	96.7	0.19	10.4	37.6 (Cu)	—	0.29 (32.3)
Cu/MWCNTs ^e	110.6	0.24	10.8	15.0 (Cu)	—	0.55 (17.1)
Ru/MWCNTs	124.2	0.24	10.9	5.0 (Ru)	0.27 (4.5)	—
Cu–Ru/MWCNTs	96.4	0.17	10.5	28.4 (Cu), 4.8 (Ru)	0.89 (1.2)	0.51 (18.4)

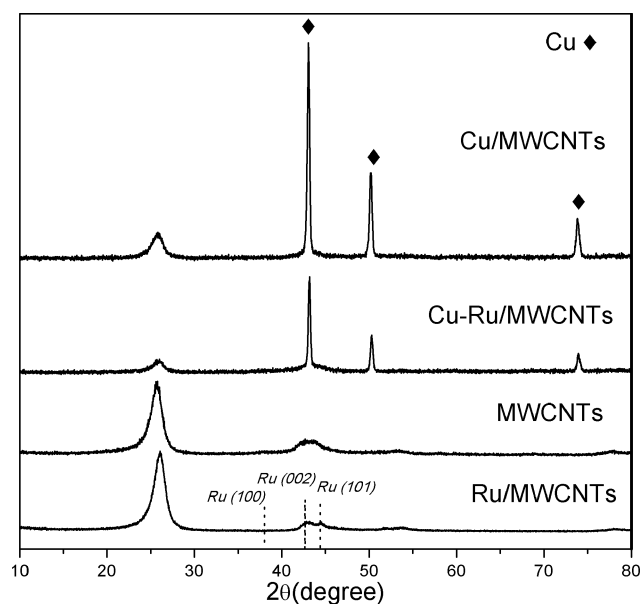
^a BET surface area calculated from the linear part of the BET plot. ^b Estimated using the adsorption branch of the isotherm by the BJH method. ^c BJH average pore size (4 V/A). ^d Mean cluster sizes were estimated from metal dispersions by assuming spherical structures and values for the atomic volume in bulk Ru (13.65×10^{-3} nm³) and Cu (11.83×10^{-3} nm³).²² ^e The catalyst was prepared by incipient wetness impregnation, dried at 373 K for 12 h, treated in dry air at 300 °C for 4 h, followed by H₂ at 300 °C for 2 h.

a good support for hydrogenation catalysts because of their excellent hydrogen adsorption,¹² especially carbon nanotubes, which have been regarded as a potential hydrogen storage medium *via* hydrogen spillover.¹³ Here, we report a simple route to the synthesis of carbon nanotube decorated with Cu–Ru bimetallic nanoparticles for glycerol hydrogenolysis. In this route, the Cu decorated carbon nanotubes were prepared by a rapid, solventless, bulk preparation method,¹⁴ and Ru metal was introduced by the chemical replacement method.

Results and discussion

Catalyst characterization

The structure of catalysts was characterized by the X-ray diffraction (XRD) patterns as shown in Fig. 1. Two broad and featureless peaks at $2\theta = 26$ and 43° are observed in the XRD pattern of the multi-wall carbon nanotubes (MWCNTs). For the Cu/MWCNTs sample, the peaks at $2\theta = 43$, 50 and 74° correspond to the presence of Cu metal (JCPDS No. 1-1241).

**Fig. 1** XRD patterns of samples.

The Cu–Ru/MWCNTs show only the peaks corresponding to Cu metal, and no reflections corresponding to Ru metal are detected. This can be ascribed to the occurrence of highly dispersed Ru species by the chemical replacement method,^{6,19} in which the Ru³⁺ cations selectively replace surface copper atoms, especially the active sites (defects, vacancies, *etc.*), resulting in discontinuous Ru metal species. However, a weak peak corresponding to the (101) plane of Ru metal could be distinguished in the XRD pattern of Ru/MWCNTs (JCPDS No. 1-1253), suggesting larger Ru clusters. It is reasonable to speculate that the Ru metal species should be selectively located on the surface of Cu metal nanoparticles to generate tiny Ru clusters.

Table 1 shows the surface properties of the catalysts. The BET surface area, pore volume and pore size of MWCNTs change a bit after the deposition of metal onto the supports. The Cu/MWCNTs sample shows a much lower surface area and pore volume than Ru/MWCNTs, owing to the higher Cu metal loading. After the replacement of Cu/MWCNTs with Ru³⁺, the resulting Cu–Ru/MWCNTs catalyst exhibits a similar surface area and pore properties to the Cu/MWCNTs. This indicates that the deposition of Ru clusters should mainly occur on the surface of Cu metal without any influence on the carbon surface. Moreover, the dispersion of active Cu metal increases 76% after the replacement (Table 1), which comes from the ~40% decrease of Cu particle size as shown in Fig. 2. Compared to the Ru/MWCNTs sample, the Cu–Ru/MWCNTs sample shows higher Ru metal dispersion (1.6 times), suggesting that the Ru clusters are highly dispersed on the surface *via* chemical replacement and the capability of hydrogen activation is enhanced.¹⁴ Fig. 2 shows the transmission electron microscope (TEM) images of the support and metal catalysts. Most of the Ru, Cu and Cu–Ru particles are located on the external surface of the MWCNTs without incorporating clusters into the pores of MWCNTs. ~35 nm Cu particles are highly dispersed over the surface of MWCNTs, and smaller Ru particles (~5 nm) are also distributed homogeneously in the Ru/MWCNTs samples. After the deposition of Ru by the chemical replacement between Cu nanoparticles and Ru³⁺ cations, the size of Cu–Ru particles decreases to ~20 nm. The location of Ru on the surface of Cu nanoparticles is confirmed by the EELS mapping and EDS analysis (Fig. S1†). As confirmed by the chemisorption results (Table 1), the decrease of particle size after replacement results in a higher Cu metal dispersion.

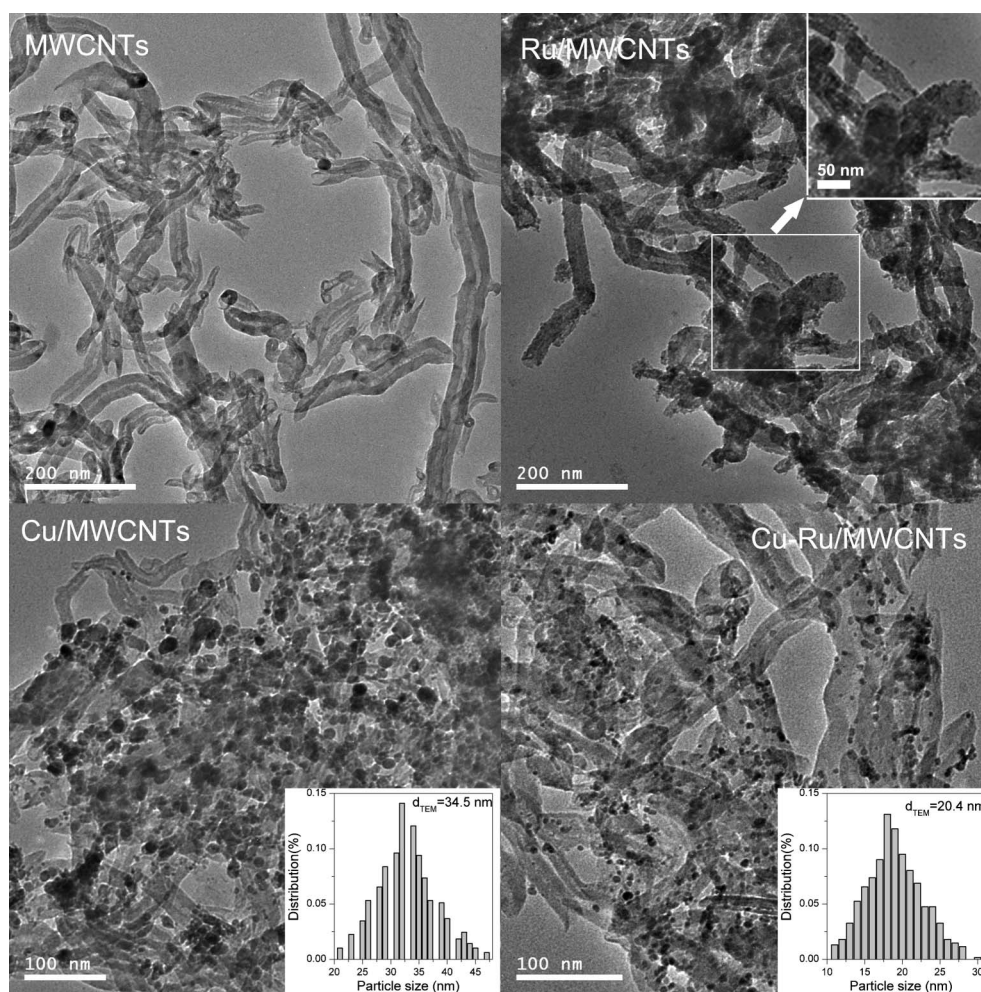


Fig. 2 TEM images and particle size distribution graphs of metal (Cu and Cu–Ru) clusters. The surface-area-weighted particle size distribution, d_{TEM} , was calculated from $d_{\text{TEM}} = \sum n_i d_i^3 / \sum n_i d_i^2$.^{11c}

In our previous work, the surface alloying effect or surface interaction between added metals and host metals occurred in bimetallic nanoparticles prepared by the chemical replacement method.¹¹ Here, the surface interaction between Ru and Cu metal was measured by the X-ray photoelectron spectroscopy (XPS) characterization. Fig. 3 shows the XPS spectra of Ru/MWCNTs, Cu/MWCNTs and Cu–Ru/MWCNTs samples. The binding energies of Ru in Ru/MWCNTs are 280.5 eV (Ru 3d_{5/2}), 461.7 eV (Ru 3p_{3/2}) and 484.1 eV (Ru 3p_{1/2}), suggesting the presence of elemental Ru at the external surface of catalyst.^{10,15} The binding energies of Cu in Cu/MWCNTs are 932.8 eV (Cu 2p_{3/2}) and 952.6 eV (Cu 2p_{1/2}), corresponding to the presence of surface metallic Cu species.¹⁶ The binding energy of C 1s (284.7 eV) on Ru/MWCNTs is the same as that of Cu/MWCNTs. For the Cu–Ru/MWCNTs catalyst, the binding energies of Ru, Cu and C do not shift compared with Cu/MWCNTs and Ru/MWCNTs, suggesting no obvious surface interaction of Ru and Cu occurs after the replacement.

Catalytic performance

Table 2 summarizes the results of glycerol hydrogenolysis. For the hydrogenolysis of glycerol, 1,2-PDO, ethylene glycol (EG),

1-propanol, 2-propanol, ethanol and methanol were detected in the liquid products, and CH₄ was the main product in the gas phase. When Ru/C and Ru/MWCNTs catalysts were used (Table 2), the conversions of glycerol were 55.7% and 65.5%, respectively. For both Ru metal catalysts, cleavage of C–C bonds was observed, and CH₄ was detected as the main gas product, the yield of liquid product being ~70%. In addition, the content of EG in the liquid product was 7–15%, which is high compared with the results using Cu and Cu–Ru catalysts (listed in Table 2). EG is formed by cleavage of the C–C bond, further demonstrating that Ru is active in the cleavage of the C–C bonds, which is in agreement with the work of other groups.⁶ In contrast, the Cu/MWCNTs catalyst exhibited lower hydrogenolysis rate and conversion of glycerol (31.3%), but ~100% yield of liquid product, and an especially high selectivity for 1,2-PDO (Table 2), indicating that Cu catalysts have poor activity towards C–C bond cleavage and good activity towards C–O bond hydrogenation. For Cu catalysts with different Cu crystallite sizes ranging from 32 to 17 nm (Table 1), their activities tended to increase inversely from 1.2×10^{-3} to 1.8×10^{-3} mol_{glycerol} mol⁻¹ surface-metal s⁻¹ (Table 2), suggesting the size requirement of active sites in which the high hydrogenolysis activity occurs on the large clusters. When the Cu/MWCNTs

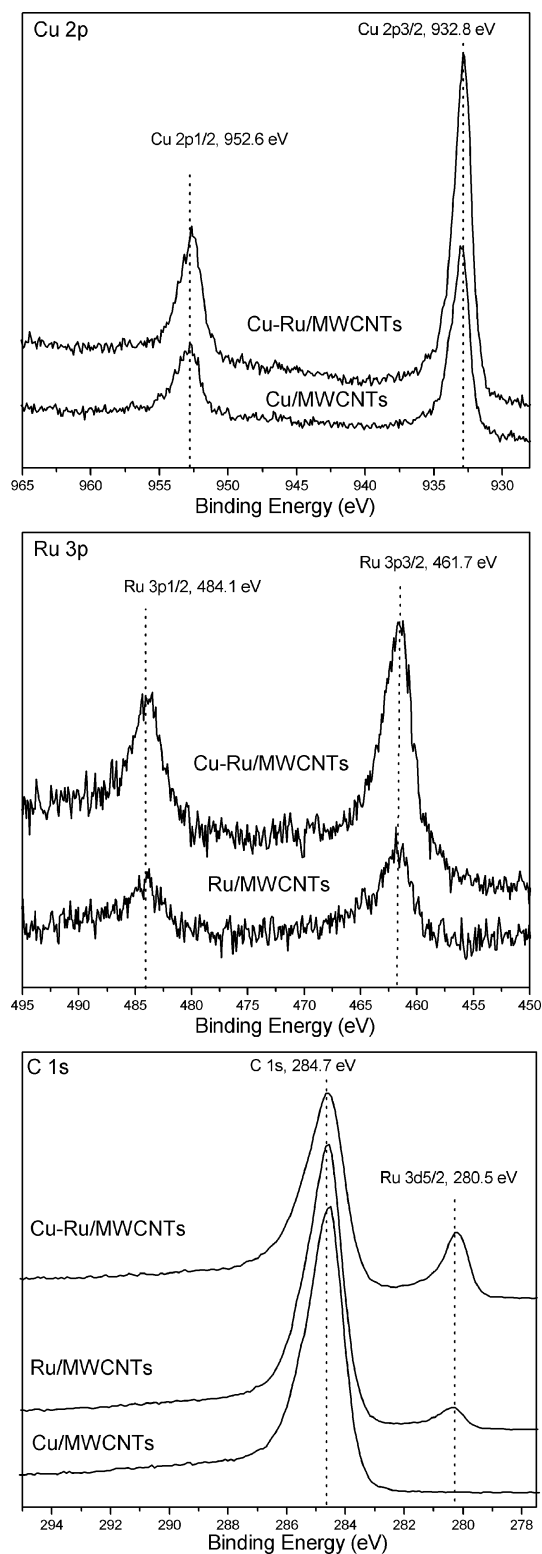


Fig. 3 XPS spectra of samples.

and Ru/MWCNTs were mixed together and used to catalyze the hydrogenolysis, about 10% increase of glycerol conversion occurred relative to Ru/MWCNTs, and 73.7% yield of liquid and 74.2% selectivity of 1,2-PDO were found, which is similar to that of the Ru/MWCNTs. This suggests the Ru/MWCNTs contributed the most activity in the mixture of catalysts. For

the Cu–Ru/MWCNTs catalysts, it is interesting to find that the conversion of glycerol increases by ~60% compared with Ru/MWCNTs, and 99.7% yield of liquid product and 86.5% selectivity to 1,2-PDO were found, which are close to that of Cu metals.

Discussion

For the glycerol hydrogenolysis, unsaturated species adsorbed on Cu undergo nucleophilic attack, which lead to dehydroxylation (C–O cleavage), and retro-Michael (C–C cleavage) reactions. The latter reaction makes it possible to obtain the selective conversion of glycerol to ethanol and glycols, but it is always less competitive than dehydroxylation.^{4,6} Therefore, the Cu catalyst shows high selectivity for the dehydroxylation products (1,2-PDO, 1-propanol, 2-propanol) as shown in Table 2.¹² On the other hand, the C–C bond hydrogenolysis on Ru metal could easily lead to the C₂ and C₁ products, and higher selectivities of ethanol, methanol and methane are observed on Ru catalysts.

As confirmed by XPS characterization above, no obvious interaction of Cu and Ru occurred in the Cu–Ru/MWCNTs catalyst, suggesting that the Ru and Cu could not greatly influence the hydrogenolysis properties of each other. The high yield of liquid product and 1,2-PDO selectivity (Table 2) on Cu–Ru catalyst are generated by the Cu metal, because the Cu metal is not able to hydrogenolyze C–C and C–O bonds, but presents hydro-dehydrogenating properties toward C–O bonds.^{4,6} The Ru metal shows high activity of C–C cleavage reactions (Table 2), resulting in high yield of CH₄. The results show that the hydrogenolysis of glycerol should not directly occur on Ru metal of Cu–Ru/MWCNTs catalyst.

The hydrogenolysis of glycerol reaction has been regarded as a structure-sensitive reaction.^{4,17,18} The activity is dependent on the particle size, and large Cu crystallites⁴ and Ru crystallites (Table S1†) generally exhibit a high glycerol hydrogenolysis rate. The Cu–Ru catalyst was prepared by the chemical replacement method, suggesting that the size of Ru clusters is influenced by the Cu particle sizes because the Ru species are located on the surface of Cu nanoparticles.^{11c} For metal nanoparticles, the facets with different surface free energies show different activities for the metal ions replacement during the chemical replacement reaction.¹⁹ This indicates that, to deposit the Ru on the Cu metal surface by replacement, the dissolution of Cu and the deposition of Ru could not occur uniformly on the surface of Cu particles. This makes it difficult to obtain a continuous Ru film or large Ru clusters on the surface of Cu particles, suggesting that the Cu acts as the diluting element to inhibit the growth of Ru particles/film. This dilution selectively poisons the hydrogenolysis reaction, which requires relatively large clusters or ensembles of adjacent Ru atoms.²⁰ The highly dispersed Ru metal species at the external surface of Cu particles make it difficult to adsorb (and activate) glycerol in the hydrogenolysis reaction.

Compared to the Cu/MWCNTs, the derived Cu–Ru catalyst shows more than double the hydrogenolysis rate (turnover rate, TOR) and conversion of glycerol. For the replacement of Cu metal with Ru³⁺ ions, the particle size of Cu particles decreases by ~45%, resulting in an increase of 30% of the amount of surface-active Cu metal per gram of catalyst. On the other hand, the

Table 2 Glycerol hydrogenolysis rates, conversion, yields and selectivities

Sample	Conversion (%)	TOR (10^{-3} mol mol^{-1} $\text{surface-metal}^{-1}$ s^{-1}) ^a	Liquid yield (%)	Selectivities of liquid product (mol%)					
				1,2-Propanediol	1-Propanol	2-Propanol	Glycol	Ethanol	Methanol
Ru/C	55.7	61.1 (Ru)	71.3	59.4	5.8	2.0	15.7	1.1	16.0
Cu/MWCNTs	31.3	1.8 (Cu)	~100 ^b	91.1	3.2	4.0	0.2	0.2	0.5
Cu/MWCNTs ^c	15.5	1.2 (Cu)	~100	90.7	3.5	3.2	0.1	0.1	0.1
Ru/MWCNTs	65.5	55.2 (Ru)	72.2	71.2	7.5	3.2	7.6	2.2	8.3
Cu/MWCNTs + Ru/MWCNTs ^d	77.2	60.6 (Ru)	73.7	74.2	2.2	1.5	9.6	3.4	9.1
Cu–Ru/MWCNTs	99.8	3.9 (Cu)	99.7	86.5	10.4	2.9	0.1	0	0.1

^a Reaction activities were reported as the turnover rate (TOR) at ~5% conversion of glycerol, which is defined as the molar glycerol conversion rates per mole of surface metal atoms (estimated from surface titration by CO and H₂ gas described above). ^b The gas product of hydrocarbons is under the detection limit of the TCD detector of GC. ^c The catalyst was prepared by incipient wetness impregnation, dried at 373 K for 12 h, treated in dry air at 300 °C for 4 h, followed by H₂ at 300 °C for 2 h. ^d The catalyst was prepared by manual mixing of Cu/MWCNTs and Ru/MWCNTs using a mortar and pestle. The mounts of Cu and Ru used in the mixture are the same as those in the Cu–Ru/MWCNTs sample.

Cu–Ru catalyst also shows much higher (~3 times, in Table 2) TOR than that of Cu/MWCNTs with similar metal crystallite sizes (~20 nm in Table 1). These results show that the high increase in conversion and TORs after deposition of Ru on the surface of Cu metal does not mainly result from the decrease of Cu particle size, and the presence of highly dispersed Ru metal should play a more important role. Although the Ru on the Cu–Ru cannot activate the glycerol molecules, it clearly dissociates the hydrogen molecule to active hydrogen atoms, which is confirmed by the hydrogen chemisorption result (Table 1). In the hydrogenolysis of glycerol on Cu–Ru catalyst, the presence of Ru acts as a route for the spillover of hydrogen toward the major catalytic component, Cu, making it a highly active catalyst.²¹ The use of spillover hydrogen has also been reported by Zhou *et al.*,^{7d} in which the hydrogen was activated by Ag metal to reduce CuO into active Cu metal. Here, the hydrogen activated by Ru metal diffuses over Cu metal surface nearby, which increases the concentration of active hydrogen accessing the adsorbed glycerol molecule.

In the present work, highly dispersed Ru clusters on Cu nanoparticles have been prepared by the chemical replacement method using Cu nanoparticles and Ru³⁺ ions. The resulting Ru metal clusters provide active hydrogen on the surface of the Cu nanoparticles, increasing the hydrogenolysis activity of Cu metal.

Conclusions

The nanotube-supported Cu–Ru nanoparticles were prepared by the chemical replacement method, in which the Ru species were located on the external surface of Cu nanoparticles. The deposition of Ru on the surface of Cu particle reduced the Cu particle size and promoted the hydrogen activation ability of Cu metal. Although the Ru in Cu–Ru could not catalyze the hydrogenolysis of glycerol, it acted as a route for hydrogen spillover. The resulted Cu–Ru catalyst showed higher 1,2-PDO selectivity than that of the Ru catalyst, and better activity than the Cu catalyst. This study shows that chemical replacement is a powerful method to prepare catalysts with high activity and selectivity by the surface modification of metal nanoparticles.

Experimental

Chemicals

Multi-walled carbon nanotubes (MWCNTs, diameter 15–45 nm) were obtained from Xiamen University. Copper(II) acetate (98%), ruthenium trichloride (99.995%) and 5 wt.% Ru/carbon catalysts were purchased from KRS Fine Chemical Co. Ltd (Tianjin, China), and used as received.

Catalyst preparation

The synthesis of Cu nanoparticle-decorated MWCNTs followed the work of Lin.¹⁴ In a typical manual mixing experiment with 10 mol% Cu loading, MWCNTs (1.0 g, ~0.083 mole carbon equivalent) were dry-mixed with powdered Cu(OAc)₂·H₂O (1.8 g, ~9 mmol) using a mortar and pestle until homogenous (30 min) under ambient conditions. The solid Cu(OAc)₂/MWCNT mixture was then transferred to a glass vial and heated in an Ar flow (100 cm³ g⁻¹ min⁻¹) to 300 °C with a ramping rate of 2 °C min⁻¹, and held isothermally for 3 h. The product (Cu/MWCNTs) was then collected without exposing it to air.

The Ru–Cu/MWCNTs was prepared by the replacement method based on our previous work.¹¹ In a typical experiment, the freshly prepared Cu/MWCNTs (without contact with air) was added to the 0.01 mol L⁻¹ RuCl₃ solution under flowing Ar gas (40 cm³ g⁻¹ min⁻¹). After replacement, the sample was washed thoroughly until no Cl⁻ was detected using 0.1 mol L⁻¹ AgNO₃ solution. The collected sample was dried in an Ar flow (100 cm³ g⁻¹ min⁻¹) at 80 °C for 12 h, and then treated in a 20% H₂/Ar flow (100 cm³ g⁻¹ min⁻¹) at 300 °C for 1.0 h. The Ru loading was selected as 5 wt.%. For comparison, 5 wt.% Ru/MWCNTs was prepared by incipient wetness impregnation of aqueous RuCl₃ solutions onto MWCNTs. The sample was treated in an air flow (100 cm³ g⁻¹ min⁻¹) at 300 °C for 3 h and subsequently reduced under 20% H₂/Ar flow (100 cm³ g⁻¹ min⁻¹) at 300 °C for 2 h.

Catalyst characterization

The chemical compositions of the samples were analyzed by inductively coupled plasma atomic emission spectrometry (ICP-AES) on an IRIS Intrepid spectrometer. The XRD patterns

of reduced samples were recorded on a Rigaku D/max 2500 X-ray diffractometer (Cu-K α , $\lambda = 1.54178 \text{ \AA}$). TEM images were acquired using a FEI Tecnai G2 high-resolution transmission electron microscope operating at 200 kV. X-ray photoelectron spectroscopy (XPS) analysis of the catalysts was carried out using a Kratos Axis Ultra DLD spectrometer employing a monochromatic Al-K α source, hybrid magnetic/electrostatic optics, and a multi-channel plate and delay line detector (DLD). The surface of the samples was etched with Ar⁺ ions for 10 min prior to removing the oxidized layer. The specific surface areas, average pore volume, and pore size distribution were measured by N₂ adsorption/desorption with the BET method on a Micromeritics ASAP 2010 C analyzer. The dispersion of metal crystallites Ru was measured using H₂ chemisorption (ASAP2020, Micromeritics) at 40 °C and 5.0–50 kPa. Samples were first treated in pure H₂ for 1 h at 300 °C and then in a dynamic vacuum for 1 h at 300 °C. The Cu metal dispersion was measured by the CO chemisorptions at 40 °C and 5.0–50 kPa. Metal dispersions were calculated by assuming H/Ru_s = 1 and CO/Cu_s = 1 stoichiometries. Mean cluster sizes were estimated from these dispersions by assuming spherical structures and values for the atomic density in bulk Ru ($13.65 \times 10^{-3} \text{ nm}^3$) and Cu ($11.83 \times 10^{-3} \text{ nm}^3$).²²

Glycerol hydrogenolysis

The glycerol hydrogenolysis reaction was carried out in a 100 mL stainless steel autoclave at a stirring speed of 800 rpm. 16 g glycerol diluted with 4 mL deionized water (80 wt.% glycerol in the aqueous solution) and 0.8 g catalyst was added to the autoclave. The reactor was sealed and purified repeatedly with hydrogen to eliminate air. Then the reactor was heated to the reaction temperature (200 °C) and pressurized to 4.0 MPa. After 6 h, the reactor was cooled to room temperature. The liquid-phase products were analyzed by a gas chromatograph with a capillary column PEG 20 M (40 m \times 3 mm \times 0.25 μm) and a flame ionization detector (FID). The gas products were detected by using a thermal conductivity detector (TCD). Conversion of glycerol is defined as the ratio of the number of moles of glycerol consumed in the reaction to the total moles of glycerol initially added. Yield of liquid product is defined as the ratio of the number of moles of glycerol consumed to produce the liquid product to the number of moles of converted glycerol. The composition of liquid product was calculated based on the number of C-based moles of each component in the liquid product.

Acknowledgements

The present work was supported by the Natural Sciences Foundation of Tianjin (10JCYBJC04400) and MOE (IRT-0927).

References

- (a) J. N. Chheda, G. W. Huber and J. A. Dumesic, *Angew. Chem., Int. Ed.*, 2007, **46**, 7164; (b) C. H. Zhou, J. N. Beltramini, Y. X. Fan and G. Q. Lu, *Chem. Soc. Rev.*, 2008, **37**, 527; (c) A. Brandner, K. Lehnert, A. Bienholz, M. Lucas and P. Claus, *Top. Catal.*, 2009, **52**, 278; (d) D. A. Simonetti and J. A. Dumesic, *Catal. Rev. Sci. Eng.*, 2009, **51**, 441; (e) Y. Gu and F. Jérôme, *Green Chem.*, 2010, **12**, 1127; (f) F. Jérôme, Y. Poulous and J. Barrault, *ChemSusChem*, 2010, **1**, 586.
- J. Sabadie, D. Barthomeuf, H. Charcosset and G. Descotes, *Bull. Soc. Chim. Fr.*, 1981, **7–8**, 288.
- A. Wawrzetz, B. Peng, A. Hrabar, A. Jentys, A. A. Lemonidou and J. A. Lercher, *J. Catal.*, 2010, **269**, 411.
- S. Wang, Y. Zhang and H. C. Liu, *Chem. Asian J.*, 2010, **5**, 1100.
- (a) M. Balaraju, V. Rekha, P. S. S. Prasad, R. B. N. Prasad and N. Lingaiah, *Catal. Lett.*, 2008, **126**, 119; (b) L. Huang, Y. L. Zhu, H. Y. Zheng, Y. W. Li and Z. Y. Zeng, *J. Chem. Technol. Biotechnol.*, 2008, **83**, 1670–1675; (c) Z. W. Huang, F. Cui, H. X. Kang, J. Chen and C. G. Xia, *Appl. Catal. A*, 2009, **366**, 288; (d) L. Y. Guo, J. X. Zhou, J. B. Mao, X. W. Guo and S. G. Zhang, *Appl. Catal. A*, 2009, **367**, 93; (e) S. Sato, M. Akiyama, K. Inui and M. Yokota, *Chem. Lett.*, 2009, **38**, 560; (f) Q. J. Yu, X. H. Ma, Z. Lan, M. Z. Wang and C. J. Yu, *J. Phys. Chem. C*, 2009, **113**, 6969; (g) A. Bienholz, F. Schwab and P. Claus, *Green Chem.*, 2010, **12**, 290.
- (a) J. Barbier, J. C. Menezes, C. Montassier, J. Naja, G. D. Angel and J. M. Dominguez, *Catal. Lett.*, 1992, **14**, 37; (b) C. Montassier, J. C. Menezes, J. Moukolo, J. Naja, L. C. Hoang, J. Barbier and J. P. Boitiaux, *J. Mol. Catal.*, 1991, **70**, 65; (c) C. Montassier, J. C. Menezes, L. C. Hoang, C. Renaud and J. Barbier, *J. Mol. Catal.*, 1991, **70**, 99; (d) C. Montassier, J. C. Menezes, J. Naja, J. Barbier, J. M. Dominguez, P. Sarrazin and B. Didillon, *J. Mol. Catal.*, 1994, **91**, 107; (e) C. Montassier, J. C. Menezes, J. Naja, J. Barbier, J. M. Dominguez, P. Sarrazin and B. Didillon, *J. Mol. Catal.*, 1994, **91**, 119.
- (a) C. H. Liang, Z. Q. Ma, L. Ding and J. S. Qiu, *Catal. Lett.*, 2009, **130**, 169; (b) N. D. Kim, S. Oh, J. B. Joo, K. S. Jung and J. Yi, *Top. Catal.*, 2010, **53**, 517; (c) R. B. Mane, A. M. Hengne, A. A. Ghalwadkar, S. Vijayanand, P. H. Mohite, H. S. Potdar and C. V. Rode, *Catal. Lett.*, 2010, **135**, 141; (d) J. X. Zhou, L. Y. Guo, X. W. Guo, J. B. Mao and S. G. Zhang, *Green Chem.*, 2010, **12**, 1835.
- (a) E. P. Maris and R. J. Davis, *J. Catal.*, 2007, **249**, 328; (b) T. Miyazawa, S. Koso, K. Kunimori and K. Tomishige, *Appl. Catal. A*, 2007, **329**, 30; (c) T. Miyazawa, S. Koso, K. Kunimori and K. Tomishige, *Appl. Catal. A*, 2007, **318**, 244; (d) M. Balaraju, V. Rekha, B. Devi, R. B. N. Prasad, P. S. S. Prasad and N. Lingaiah, *Appl. Catal. A*, 2010, **384**, 107; (e) L. Zhao, J. H. Zhou, Z. J. Sui and X. G. Zhou, *Chem. Eng. Sci.*, 2010, **65**, 30.
- (a) E. P. Maris, W. C. Ketchie, M. Murayama and R. J. Davis, *J. Catal.*, 2007, **251**, 281; (b) L. Ma and D. H. He, *Top. Catal.*, 2009, **52**, 834.
- T. Jiang, Y. X. Zhou, S. G. Liang, H. Z. Liu and B. X. Han, *Green Chem.*, 2009, **11**, 1000.
- (a) Z. J. Wu, M. H. Zhang, Z. F. Zhao, W. Li and K. Y. Tao, *J. Catal.*, 2008, **256**, 323; (b) Z. F. Zhao, Z. J. Wu, L. X. Zhou, M. H. Zhang, W. Li and K. Y. Tao, *Catal. Commun.*, 2008, **9**, 2191; (c) Z. J. Wu, Z. F. Zhao and M. H. Zhang, *ChemCatChem*, 2010, **2**, 1606.
- L. Chen, A. C. Cooper, G. P. Pez and H. S. Cheng, *J. Phys. Chem. C*, 2007, **111**, 18995.
- (a) J. M. Planeix, N. Coustel, J. Coq, V. Brotons, P. S. Kumbhar, R. Dutartre, P. Geneste, P. Bernier and P. M. Ajayan, *J. Am. Chem. Soc.*, 1994, **116**, 7935; (b) A. J. Lachawiec Jr., G. Qi and R. T. Yang, *Langmuir*, 2005, **21**, 11418.
- Y. Lin, K. A. Watson, M. J. Fallbach, S. Ghose, J. G. Smith Jr., D. M. Delozier, W. Cao, R. E. Crooks and J. W. Connell, *ACS Nano*, 2009, **3**, 871.
- R. Koetz, H. J. Lewrenz and S. Stucki, *J. Electrochem. Soc.*, 1983, **130**, 825.
- J. Hedman, M. Klasson, R. Nilsson, C. Nordling, M. F. Sorokina, O. I. Kljushnikov, S. A. Nemnonov, V. A. Trapeznikov and V. G. Zyrarov, *Phys. Scr.*, 1971, **4**, 195.
- A. Marinoiu, G. Ionita, C. L. Gáspár, C. Cobzaru and S. Oprea, *React. Kinet. Catal. Lett.*, 2009, **97**, 315.
- T. Miyazawa, S. Koso, K. Kunimori and K. Tomishige, *Appl. Catal. A*, 2007, **18**, 244.
- Q. B. Zhang, J. P. Xie, J. Y. Lee, J. X. Zhang and C. Boothroyd, *Small*, 2008, **4**, 1067.
- (a) Z. J. Wu, S. H. Ge, M. H. Zhang, W. Li, S. C. Mu and K. Y. Tao, *J. Phys. Chem. C*, 2007, **111**, 8587; (b) Z. J. Wu, M. H. Zhang, W. Li, S. C. Mu and K. T. Tao, *J. Mol. Catal. A*, 2007, **273**, 277.
- T. Inui, Y. Ono, Y. Takagi and J. B. Kim, *Appl. Catal. A*, 2000, **202**, 215.
- G. Bergeret and P. Gallezot, 'Character 3.1.2 Particle Size and Dispersion Measurements', in *Handbook of Heterogeneous Catalysis*, ed. G. Ertl, H. Knozinger, F. Schuth and J. Weitkamp, Wiley-VCH, 2008, pp. 738–745.